Active Site Specific Cadmium(II)-Substituted Horse Liver Alcohol Dehydrogenase: Crystal Structures of the Free Enzyme, Its Binary Complex with NADH, and the Ternary Complex with NADH and Bound *p*-Bromobenzyl Alcohol†

Gunter Schneider,‡,§ Eila Cedergren-Zeppezauer,‡ Stefan Knight,‡ Hans Eklund,‡ and Michael Zeppezauer*,§

Department of Molecular Biology, Biomedical Center, University of Agricultural Sciences, S-75124 Uppsala, Sweden, and Fachbereich Analytische und Biologische Chemie, Universität des Saarlandes, D-6600 Saarbrücken, West Germany

Received January 28, 1985; Revised Manuscript Received June 21, 1985

ABSTRACT: Three crystal structures have been determined of active site specific substituted Cd(II) horse liver alcohol dehydrogenase and its complexes. Intensities were collected for the free, orthorhombic enzyme to 2.4-Å resolution and for a triclinic binary complex with NADH to 2.7-Å resolution. A ternary complex was crystallized from an equilibrium mixture of NAD^+ and *p*-bromobenzyl alcohol. The microspectrophotometric analysis of these single crystals showed the protein-bound coenzyme to be largely NADH, which proves the complex to consist of Cd^{II}-LADH, NADH, and *p*-bromobenzyl alcohol. Intensity data for this abortive ternary complex were collected to 2.9-Å resolution. The coordination geometry in the free Cd(II)-substituted enzyme is highly similar to that of the native enzyme. Cd(II) is bound to Cys-46, Cys-174, His-67, and a water molecule in a distorted tetrahedral geometry. Binding of coenzymes induces a conformational change similar to that in the native enzyme. The interactions between the coenzyme and the protein in the binary and ternary complexes are highly similar to those in the native ternary complexes. The substrate binds directly to the cadmium ion in a distorted tetrahedral geometry. No large, significant structural changes compared to the native ternary complex with coenzyme and *p*-bromobenzyl alcohol were found. The implications of these results for the use of active site specific Cd(II)-substituted horse liver alcohol dehydrogenase as a model system for the native enzyme are discussed.

Cadmium has been of considerable interest as a probe of the metal binding sites in a variety of zinc enzymes (Bertini & Luchinat, 1983). The replacement of the zinc ions in the dimeric horse liver alcohol dehydrogenase (LADH)[1] by other divalent cations such as Cd(II) has been complicated by the fact that this enzyme contains two zinc ions per subunit, bound in two sites with different properties and functions. Attempts to substitute Zn(II) by Cd(II) resulted in three different species: the fully substituted Cd(II) enzyme (Sytkowski & Vallee, 1979), the enzyme with only the noncatalytic zinc ions replaced by Cd(II) (Sytkowski & Vallee, 1979), and the active site specific Cd(II)-substituted species (Anderson, 1980; Andersson et al., 1982).

Cd(II)-substituted LADHs have been used mainly in two ways for elucidating the function of the catalytic metal ion and gaining mechanistic insights: spectroscopic studies using either ^{113}Cd(II) NMR (Bobsein & Meyers, 1981) or perturbed angular correlation of γ-rays (Andersson et al., 1982) and transient kinetic studies with the active site specific substituted Cd^{II}-LADH (Dunn et al., 1982; Gerber, 1983).

However, the usefulness of metal substitution as a probe of the function of a catalytic metal ion depends critically on the degree of structural similarity between the native enzyme and the metal-substituted species. Changes in the protein structure, especially around the active site region and the metal centers, as a consequence of metal substitution would severely restrict the use of these species as model systems for the native enzyme and question mechanistic deductions, obtained from those derivatives.

In a previous paper (Schneider et al., 1983a) we have described the results of an X-ray crystallographic study of the active site specific Co(II)-substituted LADH. The structure of Co^{II}-LADH was found to be highly similar to that of the native enzyme. Here, we report the results of an X-ray crystallographic study of Cd^{II}-LADH, its binary complex with NADH, and the ternary complex of Cd^{II}-LADH formed in an equilibrium mixture of NAD^+ and *p*-bromobenzyl alcohol.

Materials and Methods

Horse liver alcohol dehydrogenase was obtained from Boehringer, Mannheim, FRG. All steps in the preparation of enzyme samples and data collection were carried out at 4 °C.

Preparation of Enzyme. LADH was recrystallized from *tert*-butyl alcohol, and the removal of the catalytic zinc ions was performed in the crystalline state according to the method of Maret et al. (1979). The active site zinc-free enzyme $H_4Zn(n)_2$LADH had a residual specific activity of 0.5% of the native enzyme. The zinc content, determined by atomic

† This work was supported by grants from the Swedish National Science Research Council, the Deutsche Forschungsgemeinschaft, and BMFT.

* Address correspondence to this author.
‡ University of Agricultural Sciences.
§ Universität des Saarlandes.

[1] Abbreviations: LADH and Zn^{II}-LADH, native horse liver alcohol dehydrogenase (EC 1.1.1.1); Cd^{II}-, Co^{II}-, and Ni^{II}-LADH, horse liver alcohol dehydrogenase whose catalytic zinc ions have been replaced by Cd(II), Co(II), and Ni(II); $H_4Zn(n)_2$LADH, enzyme lacking the metal ions at the active sites, "n" denoting the noncatalytic metal binding site; NAD^+ and NADH, oxidized and reduced nicotinamide adenine dinucleotide; TES, 2-[[tris(hydroxymethyl)methyl]amino]ethanesulfonate; MPD, 2-methyl-2,4-pentanediol; Me_2SO, dimethyl sulfoxide; F_o, observed structure factor amplitude; F_c, calculated structure factor amplitude; DACA, *trans*-4-(*N*,*N*-dimethylamino)cinnamaldehyde; OD, optical density.

0006-2960/85/0424-7503$01.50/0

adsorption, was 1.9 mol of zinc per dimer $H_4Zn(n)_2$LADH. The insertion of Cd(II) into $H_4Zn(n)_2$LADH followed the procedure described by Andersson (1980). The specific activity of the obtained Cd^{II}-LADH, measured with the method of Dalziel (1957), was 12.0–12.5% of that of the native enzyme. The zinc and cadmium contents were determined with a Perkin-Elmer 400 atomic absorption spectrophotometer. The metal content of the prepared Cd^{II}-LADH was 2.0 mol of zinc/mol of LADH and 1.8 mol of cadmium/mol of LADH.

Crystallization. Crystallization was achieved by dialyzing enzyme samples (1 mL) against 10 mL of buffer containing the precipitant MPD. The MPD concentration was raised slowly to a final concentration of 25–30% (v/v). The free enzyme (10 mg/mL) was crystallized in 0.05 M TES buffer, pH 7.5. The crystallization of the binary complex with NADH was carried out by dialyzing enzyme samples (10 mg/mL) against 0.05 M TES, pH 7.5, containing 0.5 mM NADH. The outer solution was changed twice, before the precipitant MPD was slowly added.

The crystals of the ternary complex from an equilibrium mixture were obtained similarly as described by Eklund et al. (1982). Enzyme samples (10 mg/mL) were dialyzed against 0.05 M TES buffer, pH 7.0, containing 1.2 mM NAD^+ and 1 mM *p*-bromobenzyl alcohol. The final MPD concentration was 30%.

Microspectrophotometric Measurements. Absorption spectra of single crystals of the complex obtained with Cd^{II}-LADH from the equilibrium mixture with NAD^+ and *p*-bromobenzyl alcohol were recorded at 10 °C with an automatic Zeiss microspectrophotometer using the program λ SCAN. Unpolarized light was used. Crystals used to record the spectra and to measure enzymatic activity were taken from the same batch as those used to collect the 3.7–2.9-Å X-ray intensity data.

Data Collection and Data Processing. The intensity data were collected on a STOE four-circle diffractometer. The procedures of data collection and data processing (including Lorentz and polarization correction, absorption correction, and a correction for the time-dependent decrease in intensity) employed here have been described in detail elsewhere (Eklund et al., 1976). The allowed intensity decrease due to radiation damage was 25%. The corrected structure factor amplitudes of the orthorhombic data set were scaled against the corresponding native data set. The structure factor amplitudes for the Cd^{II}-LADH/NADH complex and the ternary complex were scaled against the data set of the ternary complex of the native enzyme, NADH, and Me_2SO (Eklund et al., 1981).

(*A*) *Orthorhombic Data Set.* The crystals of Cd^{II}-LADH were orthorhombic with cell dimensions $a = 56.0$ Å, $b = 75.2$ Å, and $c = 180.7$ Å. Thirteen crystals were used to collect the 14 697 reflections corresponding to 2.4-Å resolution. The scaled observed structure factor amplitudes of Cd^{II}-LADH were combined with phases from a refined model of the native enzyme, which has at present a crystallographic *R* factor of 22% at 2.4-Å resolution (T. A. Jones, unpublished results). Difference Fourier maps were calculated with PROTEIN (W. Steigemann) using coefficients $|F_o| - |F_c|$ and $|2F_o| - |F_c|$. The examination of the difference Fourier maps and the model building was performed on a VG 3404 interactive graphics display system using the FRODO program (Jones, 1978, 1982).

Model building was done by a stepwise procedure. Difference Fourier maps without contributions of the metal ions to the structure factor calculation were computed and used for the positioning of the Cd(II) with the help of the real-space refinement option of FRODO (Jones & Liljas, 1984). Since the strong electron density of Cd(II) at the active site complicated the interpretation of the region around the catalytic metal center, Cd(II) was included in the structure factor calculation and new difference Fourier maps were calculated. In this case, the contributions of the ligands to the catalytic metal ion were omitted in the structure factor calculation. These maps were used to position the residues, which are ligated to the Cd(II) ion. After model building, the obtained model of Cd^{II}-LADH was crystallographically refined (see below).

(*B*) *Triclinic Data Sets.* The crystals of the binary complex between Cd^{II}-LADH and NADH were triclinic with cell dimensions $a = 52.0$ Å, $b = 44.6$ Å, $c = 94.2$ Å, $\alpha = 101.9°$, $\beta = 104.5°$, and $\gamma = 72.2°$. Twenty crystals were used to collect the 20 400 reflections corresponding to 2.7-Å resolution. The scaled observed structure factor amplitudes were combined with phase angles derived from a refined model of the ternary complex of native enzyme, NADH, and Me_2SO without contributions of the inhibitor Me_2SO. This model has at present a crystallographic *R* factor of 25.6% at 2.9-Å resolution (Eklund et al., 1984). The calculation of difference Fourier maps and the stepwise procedure of model building were the same as described for the orthorhombic case. The positioning of the bound coenzyme was made from difference Fourier maps, calculated without contributions of coenzyme atoms to the structure factor calculation.

The crystals of the ternary complex of Cd^{II}-LADH were triclinic with the same cell dimensions as the binary complex. Thirteen crystals were used to collect the 16 042 reflections corresponding to 2.9-Å resolution. The scaled observed structure factor amplitudes were combined with phases calculated from a model of the ternary complex of native enzyme, NAD^+, and *p*-bromobenzyl alcohol (Eklund et al., 1982) without contributions from the bound substrate. This model has at present a crystallographic *R* factor of 23% at 2.9-Å resolution (E. Horjales and H. Eklund, unpublished results). The calculation of difference Fourier maps and the procedures of model building were the same as outlined above.

Crystallographic Refinement of Cd^{II}-LADH. The orthorhombic modification of Cd^{II}-LADH was refined by using CORELS (Sussman et al., 1977) and DERIV (Jack & Levitt, 1978). In the refinement with CORELS, only 30 amino acids around the catalytic metal sphere, including the ligands to the catalytic metal ion, were refined (residues 40–50, 60–70, and 170–180). No water molecules were included in the refinement. After refinement, a new diference Fourier map with coefficients $(|F_o| - |F_{c,model}|)\alpha_{c,model}$ was calculated and inspected.

The refinement with DERIV included the whole protein structure without any solvent molecules. After refinement, the protein model was regularized with FRODO to maintain a proper stereochemistry. A difference Fourier map with coefficients $(|F_o| - |F_{c,model}|)\alpha_{c,model}$ was calculated and inspected. Stereodiagrams were plotted on a Hewlett-Packard plotter using a plot program written by T. A. Jones.

RESULTS

Orthorhombic Structure of Cd^{II}-LADH. The most significant feature in the difference Fourier map with coefficients $|F_o| - |F_c|$ was a maximum in the electron density 8 times the standard deviation of the map at the position of the catalytic metal ion. No changes in electron density above the standard deviation were detected at the position of the noncatalytic zinc ion. From this, we interpret that the catalytic zinc ion had been replaced by the more electron-rich Cd(II) and that no significant exchange of the noncatalytic Zn(II) by Cd(II) had taken place. A difference Fourier map calculated without the

FIGURE 1: (a) Difference electron density at the position of the catalytic metal ion in the $|F_o| - |F_c|$ Fourier map of Cd^{II}-LADH. The map was calculated without any contributions of the zinc ions to the structure factor calculation. The contour level shown here is 12 times the standard deviation of the map. (b) Difference electron density at the noncatalytic zinc site in Cd^{II}-LADH. The $|F_o| - |F_c|$ Fourier map was calculated without any contributions of the zinc ions to the structure factor calculation. The contour level shown here is 8 times the standard deviation of the map.

contributions of both zinc ions to the structure factor calculation showed that the peak height was 26 times the standard deviation of the map at the catalytic metal binding site (Figure 1a). Furthermore, a maximum in the electron density 19 times the standard deviation was found at the position of the noncatalytic zinc ion (Figure 1b). Thus, the occupancy of Cd(II) at the active site is high, as judged from a comparison of the electron densities for the Cd(II) and the noncatalytic zinc ion. This agrees well with the metal content of 1.8 mol of Cd(II)/mol of LADH determined by atomic absorption spectroscopy.

The position of Cd(II) in the active site of Cd^{II}-LADH, determined with the help of the real-space refinement option of FRODO, is shifted 0.3 Å toward the substrate channel, as compared with the position of the catalytic zinc ion in the native enzyme. Cd(II) is bound to the same protein ligands as Zn(II) in the native enzyme—Cys-46, His-67, and Cys-174. No further amino acid residues are coordinated to the metal ion. Small changes in the position of the protein ligands due to the larger ionic radius of the Cd(II) ion were observed, but the geometry remains still tetrahedral.

In all difference Fourier maps, electron density was found at the position of the water molecule, which is bound as fourth ligand to the catalytic zinc ion in the native enzyme. This ligand, if present, should appear as a maximum in electron density, since it was not included in the structure factor calculation. However, the assignment of bound water molecules in the active site was made after the crystallographic refinement (see below). Inspection of the difference Fourier maps revealed no significant changes in the protein structure of Cd^{II}-LADH, as compared to the native enzyme.

Crystallographic Refinement: The Metal Sphere and Assignment of Bound Solvent. A crystallographic refinement of the Cd^{II}-LADH model was carried out, which should increase the reliability of the assignment of metal-bound solvent molecules. The starting R factor of the model was 24.6%. After one cycle of CORELS or DERIV, the R factor decreased to 24.1 or 24.2%, respectively, and a further cycle with CORELS did not change the R factor. The results of both programs used were essentially identical. Cd(II) refined to the same position, which was identical with that determined with the real-space refinement option of FRODO. The bond distances between Cd(II) and the ligands were 0.2 Å longer than the metal–ligand distances in the native enzyme (T. A. Jones, unpublished results) and the active site specific Co^{II}-substituted enzyme (Schneider et al., 1983a), regardless of the procedures used. Difference Fourier maps with coefficients $|F_o| - |F_c|$ were computed, where F_c denotes structure factors calculated from the model of Cd^{II}-LADH after refinement. These difference Fourier maps showed two features around the active site metal center. A minimum in electron density was found at the position of the Cd(II) ion, which was due to a occupancy of Cd(II) less than 100%. Furthermore, a maximum in electron density of approximately 6 times the standard deviation of the map was found 2.1 Å from the Cd(II) (Figure 2), close to the position of the metal-bound water molecule in the native enzyme. No further maxima in the close proximity of Cd(II) were found. There are thus no indications from these results of an increase in the coordination number of the catalytic metal ion after substitution of Zn(II) by Cd(II). We therefore

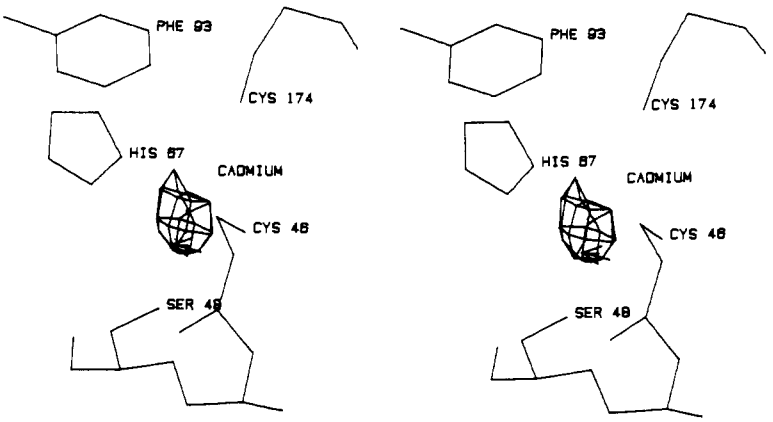

FIGURE 2: Maximum in electron density at the position of the metal-bound water molecule in Cd^{II}-LADH. The $|F_o| - |F_c|$ Fourier map was calculated after the refinement of the Cd^{II}-LADH model.

Table I: Comparison of Bond Angles between the Ligands of the Catalytic Metal Ion in Different Substituted Metallo Alcohol Dehydrogenases

ligands	angle (deg)[a]		
	Cd(II)	Co(II)[b]	Zn(II)[c]
S (Cys-174)–metal–N (His-67)	106	116	105
S (Cys-46)–metal–N (His-67)	106	100	112
S (Cys-46)–metal–S (Cys-174)	133	130	126
S (Cys-174)–metal–O (HO)	96	97	100
N (His-67)–metal–O (HO)	96	102	101
S (Cys-46)–metal–O (HO)	113	107	108

[a] The accuracy of the determination of the bond angles is estimated from the angles of the noncatalytic zinc sphere, coordinated to four sulfur atoms in a tetrahedral geometry. The root mean square deviation from a perfect tetrahedral geometry of this zinc ion is ±5° at the present resolution and stage of refinement. [b] Schneider et al. (1983a). [c] T. A. Jones (personal communication).

conclude that Cd(II) ion at the active site of Cd^{II}-LADH is bound in a distorted tetrahedral geometry with a water molecule as the fourth ligand (Table I).

Triclinic Structures. In the triclinic structures, both subunits are crystallographically independent, and the structure analysis therefore gives independent results for both subunits. At the present resolution of the map, no significant differences between the subunits were found, and we therefore present the results as relevant for both subunits.

The overall protein structure of the binary complex Cd^{II}-LADH/NADH and the ternary complex Cd^{II}-LADH/NADH/*p*-bromobenzyl alcohol is the same as that of the native ternary complexes LADH/NADH/Me_2SO (Eklund et al. 1981) and LADH/NAD^+/*p*-bromobenzyl alcohol (Eklund et al., 1982), respectively.

Binary Complex of Cd^{II}-LADH with NADH. The $|F_o| - |F_c|$ difference Fourier map, where F_o denotes the observed structure factor amplitudes of the Cd^{II}-LADH/NADH complex and F_c the calculated structure factors from the model of the native ternary complex of LADH/NADH/Me_2SO without contributions of the inhibitor Me_2SO, showed a maximum in electron density 7 times the standard deviation of the map, at the position of the catalytic metal ion. No difference in electron density above the standard deviation was found at the position of the noncatalytic zinc ion. The position of the bound Cd(II) at the active site was determined according to procedures outlined above. The contributions of both zinc ions to the structure factors, calculated from the native model, were removed, and new difference Fourier maps were computed. The $|F_o| - |F_c|$ map showed a maximum in electron density at the active site metal center of 17 times the standard deviation of the map. The position of Cd(II) in the active site of the binary complex is shifted 0.3 Å from the position of the zinc in the native ternary complex LADH/NADH/Me_2SO.

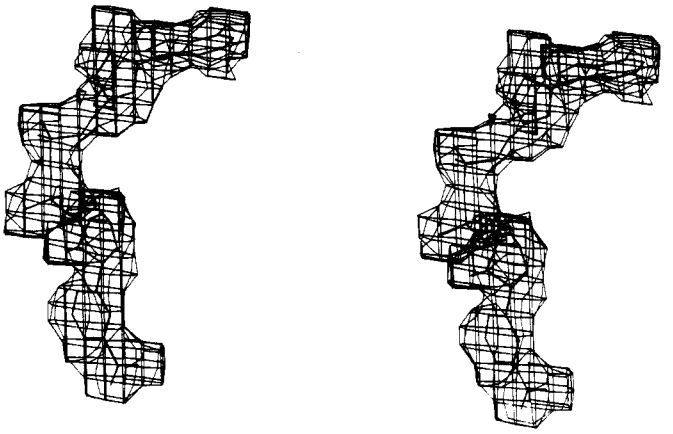

FIGURE 3: Part of a $|2F_o| - |F_c|$ Fourier map of the binary complex Cd^{II}-LADH/NADH, showing the electron density for the bound coenzyme and the superimposed model. The difference Fourier map was calculated without contributions of coenzyme atoms to the structure factor calculation.

Cd(II) was then included in a F_c calculation, and new difference Fourier maps were calculated in order to examine the active site residues. Well-defined electron density was found for the three protein ligands of the Cd(II), i.e., Cys-46, His-67, and Cys-174. Placed in their electron density, these residues provided a ligand arrangement with the three coordinating atoms on three edges of a distorted tetrahedron. The bond distances are longer than the corresponding ones in the ternary complexes of the native enzyme, but they cannot unambiguously be determined at the present resolution of the map.

The model building of the bound coenzyme was done from $|2F_o| - |F_c|$ Fourier maps, calculated without contributions from the coenzyme atoms to the structure factor calculation. Well-defined continuous electron density was found for the whole coenzyme molecule, the highest densities appearing at the positions of the phosphate groups (Figure 3). The model of NADH derived from the native LADH/NADH/Me_2SO complex could be placed into this density. Only minor adjustments of the adenine part and the nicotinamide part of the coenzyme molecule were required in order to fit this model to the observed density. The interactions of the coenzyme with the protein were essentially the same as observed in the native ternary complexes, which are described in detail elsewhere (Eklund et al., 1983, 1984). The nicotinamide ring is not

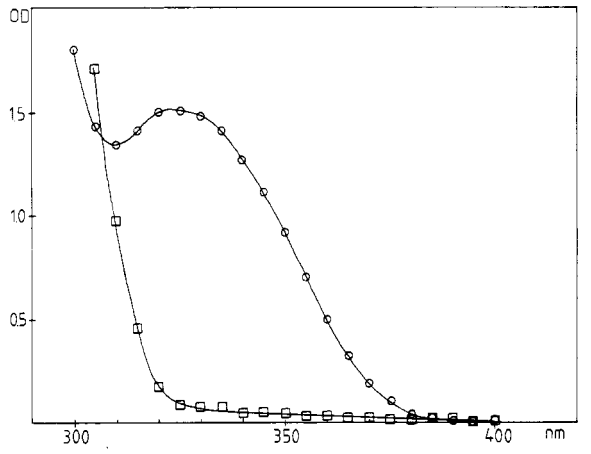

FIGURE 4: Single-crystal absorption spectra of the triclinic Cd^{II}-LADH/NADH/*p*-bromobenzyl alcohol complex: (○) spectrum of a crystal from the batch used for data collection; (□) spectrum of the same crystal after conversion into the dead-end complex by treatment with 20 mM benzaldehyde and 40 mM pyrazole.

ligated to Cd(II) but is in van der Waals contact to the catalytic metal ion. The interactions between the nicotinamide ring and the active site residues of Cd^{II}-LADH are listed in Table II.

Strong electron density was observed in the substrate channel of the binary complex Cd^{II}-LADH/NADH at a position where the precipitant MPD has been found in the native enzyme and other complexes of LADH (Plapp et al., 1978; Cedergren-Zeppezauer et al., 1982). An MPD molecule could be placed into this density, giving favorable interactions with amino acids forming the hydrophobic substrate pocket. One of the hydroxyl groups of MPD forms a hydrogen bond to the hydroxyl oxygen of Ser-48. The MPD molecule is not ligated to the catalytic metal ion since its closest oxygen is t 6-Å distance from the cadmium ion.

Ternary Complex of Cd^{II}-LADH with Coenzyme and Substrate. The difference Fourier maps, calculated with the data from the ternary complex of Cd^{II}-LADH with coenzyme and bound substrate, showed three major features, i.e., a strong spherical electron density about 9 times the standard deviation of the map for the bromine atom, a flat density about 7 times the standard deviation for the phenyl ring of the substrate molecule, and a maximum in electron density of 5 times the standard deviation at the position of the catalytic metal ion due to the substitution of Zn(II) by the more electron-rich Cd(II). The peak heights were identical in both subunits. The occupancy of the ternary complex with both *p*-bromobenzyl alcohol and Cd(II) is high, as can be estimated from a comparison of their electron densities with the electron density for the noncatalytic zinc ion. The electron density for this metal ion is 9 times the standard deviation of the map, if the contributions of the noncatalytic zinc ion to the structure factors are omitted in the F_c calculation.

Table II: Interactions of the Nicotinamide Ring with the Protein in the Binary Complex of Cd^{II}-LADH with NADH[a]

nicotinamide atom	protein atom	nicotinamide atom	protein atom
N1	none	C6-N	C_{γ^2} (Val-203)
C2-N	O (Val-292)	C7-N	none
	C_{γ^2} (Val-294)	O1-N	N (Phe-319) (HB)
C3-N	none		$C_{\gamma}1$ (Ile-318)
C4-N	S_{γ} (Cys-174)	N2	O (Ala-317) (HB)
C5-N	Cd(II)		C_{γ^1} (Ile-318)
	C_{γ^1} (Val-203)		C_{δ^1} (Ile-318)

[a] All protein atoms closer than 3.8 Å are included. HB denotes a hydrogen-bond distance (2.7–2.9 Å).

No significant differences to the native ternary complex could be observed at the present resolution of the maps. The interactions of the nicotinamide ring with the active site of Cd^{II}-LADH in the ternary complex are identical with those in the binary complex with NADH (Table II) and the native ternary complex with NAD^+ and *p*-bromobenzyl alcohol (Eklund et al., 1982).

The UV and visible spectra recorded on single crystals of the ternary complex with coenzyme and *p*-bromobenzyl alcohol are shown in Figure 4. The spectrum shows the typical absorption band at 320 nm due to bound NADH. The addition of the chromophoric substrate DACA to these crystals resulted in an intense absorption band (λ_{max} 456 nm), characteristic for the metal bound aldehyde in the presence of reduced coenzyme (Dietrich, 1980; Dunn et al., 1982). After addition of benzaldehyde and pyrazole (Bignetti et al., 1979) to the crystalline ternary complex, the absorption maximum at 320 nm decreased from 1.5 OD to 0. This demonstrates that the crystalline Cd^{II}-LADH complex does convert aldehyde. The outer solution, from which the crystals were grown, did not contain detectable amounts of NADH. The 15 crystals tested showed an absorption ratio $A_{280nm}/A_{320nm} = 4$, which indicates that virtually all coenzyme is bound as NADH.

In all difference Fourier maps, strong electron density was found for the bound *p*-bromobenzyl alcohol close to the catalytic metal center (Figure 5). By use of the real-space refinement option of the FRODO program, the positioning of the substrate in its density was straightforward. The high spherical density for the bromine atom allows a sufficiently accurate determination of its position and, consequently, a

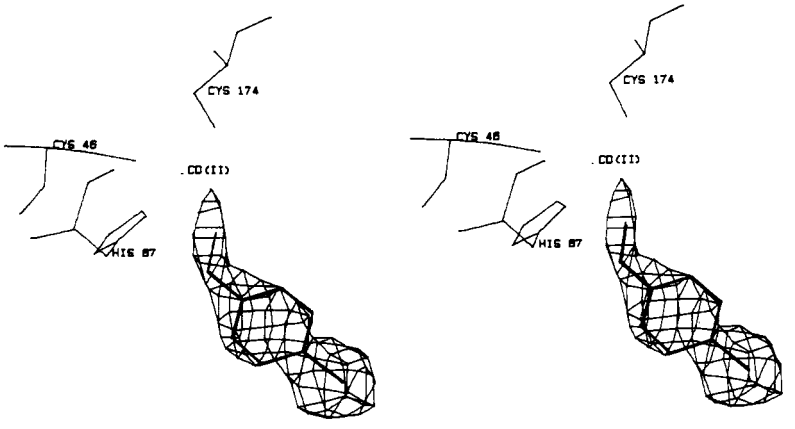

FIGURE 5: Difference electron density for the bound substrate in the ternary complex Cd^{II}-LADH/NADH/*p*-bromobenzyl alcohol. A model of the substrate is superimposed on the electron density.

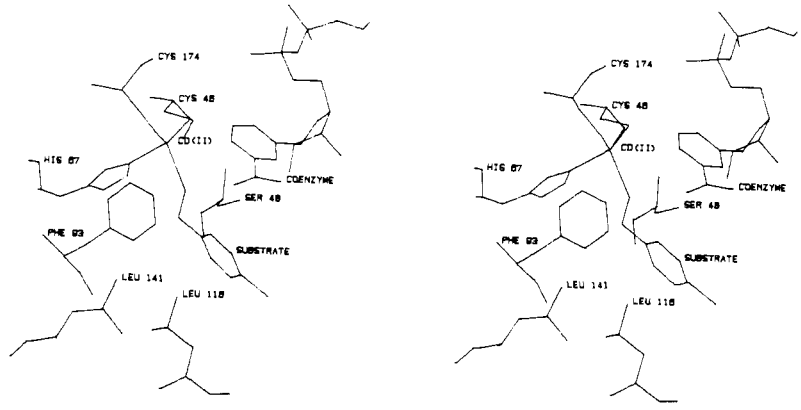

FIGURE 6: Stereodiagram of the active site in the ternary complex Cd^{II}-LADH/NADH/*p*-bromobenzyl alcohol.

Table III: Interactions of the Bound Substrate with Protein and Coenzyme Atoms[a]

substrate atom	protein/coenzyme atoms	substrate atom	protein/coenzyme atoms
O1	Ser-48: O_γ, C_β	C4	Leu-116: $C_{\delta 2}$
	His-67: $C_{\delta 2}$, $N_{\epsilon 2}$		Leu-57: $C_{\delta 2}$
	Cys-174: S_γ	C5	Leu-116: $C_{\delta 2}$
	Cd(II)		Val-294: $C_{\gamma 2}$
	coenzyme: C3-N, C4-N, C5-N, C6-N	C6	Leu-57: $C_{\delta 2}$
			Leu-116: $C_{\delta 2}$
C1	Ser-48: O_γ, C_β		Val-294: $C_{\gamma 2}$
	Cd(II)	C7	Ser-48: C_β, O_γ
	His-67: $N_{\epsilon 2}$, $C_{\delta 2}$		Leu-57: $C_{\delta 2}$
C2	Ser-48: C_β, O_γ	Br	Val-294: $C_{\gamma 2}$
C3	Ser-48: C_β, O_γ		
	Phe-93: $C_{\epsilon 2}$		

[a] All atoms closer to substrate atoms than 3.8 Å are listed.

rather accurate determination of the metal–substrate distance. When placed into its density, the distance between the substrate oxygen and the catalytic metal ion is 2.3 Å, showing direct coordination of the substrate to Cd(II). Thus, the catalytic cadmium ion is tetracoordinated with three protein ligands and the substrate oxygen atom in a distorted tetrahedral geometry. No indications of additional ligands were found in the difference Fourier maps.

Figure 6 shows the final result of the model building with the alcohol bound to the metal ion. The interactions between the substrate and protein and coenzyme atoms at the active site are listed in Table III. The observed mode of substrate binding is nonproductive, since the pro-*R* hydrogen is pointing away from the C4 atom of the nicotinamide ring. However, there is no steric hindrance for a rotation of the *p*-bromobenzyl alcohol along the C1–Br axis. Such a rotation would bring the C1 atom of the substrate into a position with the pro-*R* hydrogen close to the C4 atom of the nicotinamide ring, favorable for direct hydride transfer. A similar mode of binding has been observed in the native ternary complex with NAD^+ and *p*-bromobezyl alcohol described by Eklund et al. (1982).

DISCUSSION

The specific replacement of the catalytic zinc ions in LADH by the extraction/insertion method proceeds in two steps. The first step is the specific removal of the catalytic zinc ions. In the second step, the metal in question, e.g., Co(II), Ni(II), Cu(II), or Cd(II), is inserted into the empty catalytic metal binding site (Zeppezauer, 1983). This pathway has been proved by an X-ray crystallographic investigation of the active site specific zinc-depleted intermediate $H_4Zn(n)_2$LADH and the Co(II)-substituted enzyme (Schneider et al., 1983a). In accordance with these findings, the present study of the Cd(II)-substituted enzyme confirms the active site specific replacement of Zn(II) by Cd(II) in Cd^{II}-LADH. No exchange of the noncatalytic Zn(II) against Cd(II) has taken place, since the more electron-rich Cd(II) would have been observed readily in the difference maps if it were present in significant amounts.

The geometry of the catalytic metal center is highly preserved even after the reconstitution with Cd(II), an observation also made for the Co(II)-substituted LADH (Schneider et al., 1983a). The general increase in bond lengths by 0.2 Å between the Cd(II) ion and the liganding atoms that is observed in the free Cd^{II}-LADH is both expected from the difference in ionic radii between Cd(II) and Zn(II) ions and reasonable as judged from the refinement criteria. Table I shows a comparison of the bond angles of the catalytic metal center in the native enzyme with the Co(II)- and Cd(II)-substituted derivatives. In all cases, the metal is bound in a distorted tetrahedral geometry to the three protein ligands and a water molecule. The preservation of this ligand geometry in the Cd(II)-substituted enzyme is somewhat unexpected, since it is known from the coordination chemistry of this metal ion that Cd(II) has a marked preference for five- or six-coordination. The fact that Cd(II) is four-coordinated in LADH thus reinforces the conclusion drawn earlier from the results of the X-ray structure of the Co(II)-substituted enzyme (Schneider et al., 1983a) that the protein structure in LADH is important for the coordination geometry the active site metal acquires at its binding site.

The binding of coenzyme to LADH has been shown to induce a conformational transition from the open to the closed form of the enzyme, an important step in the catalytic pathway (Eklund + Brändén 1983). The functional significance of this conformational change is to tighten the coenzyme binding site, which makes possible more intimate protein–coenzyme interactions and closes one entrance to the active site. Simultaneously, a number of water molecules are expelled (Eklund et al., 1984). The conformational change is influenced by a number of parameters that have been discussed elsewhere (Eklund et al., 1982; Cedergren, 1984; Cedergren-Zeppezauer et al., 1982). The type of metal ion present at the active site does not affect the binding of coenzyme from a structural point of view.

This is obvious from the overall protein structure and the interactions between protein and coenzyme that are identical in the native complex with NADH and Me_2SO and in the binary complexes with NADH of the Cd(II)- and Co(II)-substituted derivatives. Furthermore, the mere presence or absence of the catalytic metal ion itself seems not to be critical for the conformational transition, since the closed protein conformation and the protein–coenzyme interactions in the

binary complex of the active site specific metal-depleted enzyme $H_4Zn(n)_2$LADH and NADH are highly similar to those of the native complex with NADH and Me_2SO (Schneider et al., 1983b). However, significant deviations in kinetic parameters of coenzyme binding between these derivatives have been observes (Dietrich, 1980; Gerber, 1983; Zeppezauer, 1983; Zeppezauer et al., 1984). Since no obvious structural changes are responsible for these kinetic differences in the coenzyme binding step, the presence and the type of metal ion at the active site must bring about changes in the environment that modulate the affinity for the coenzyme. A possible function of the metal in this context has been discussed elsewhere (Schneider et al., 1983b).

The equilibrium between *p*-bromobenzaldehyde/NADH and *p*-bromobenzyl alcohol/NAD^+ favors the alcohol by a factor more than 10:1 (Plapp et al., 1978). Since native enzyme and Cd^{II}-LADH act as catalysts for this reaction, it should not matter whether the native or the Cd(II)-substituted derivative are present in the equilibrium mixture. Neither will shift the equilibrium. The K_m values of Cd^{II}-LADH for *p*-bromobenzyl alcohol or *p*-bromobenzaldehyde are of the same order of magnitude, 170 and 360 μM, respectively (unpublished data). The ternary complex therefore contains predominantly bound alcohol. However, the affinity of LADH for oxidized and reduced coenzyme is markedly different, the reduced coenzyme binding 100 times stronger to the enzyme than the oxidized form. This applies also to the Cd^{II}-LADH (Dietrich, 1980). Due to this difference in binding constants, the enzyme present in the equilibrium mixture will act as an efficient trap for the reduced coenzyme, which is formed to a certain extent under equilibrium conditions.

This is demonstrated by the obtained single-crystal absorption spectra of the ternary complex, which prove the bound coenzyme to be NADH. Since the outer solution was shown not to contain NADH, the maximum amount of *p*-bromobenzaldehyde formed is equal to that of enzyme-bound NADH, i.e., 1.23 μmol in the experiment described under Results. Thus, the ratio of *p*-bromobenzyl alcohol to *p*-bromobenzaldehyde is 9:1 in the system. Since alcohol binds more strongly in the abortive complex with NADH than in the productive ternary complex, it is evident that our crystals obtained from the equilibrium mixture predominantly represent the abortive ternary complex Cd^{II}-LADH/NADH/*p*-bromobenzyl alcohol.

The difference Fourier maps calculated with intensity data of this ternary complex clearly show direct binding of the substrate to Cd(II). This parallels spectroscopic studies of the binding of the chromophoric substrate DACA to Cd^{II}-LADH, which indicated direct coordination to the catalytic metal ion (Dietrich, 1980; Dunn et al., 1982). In contrast, the ^{113}Cd(II) NMR data from binding studies of 2,2,2–trifluoroethanol and pyrazole to this derivative were interpreted in terms of indirect substrate binding (Bobsein + Meyers, 1981). This conclusion was based on the chemical shifts observed in the ternary complexes of the Cd(II) enzyme with NAD^+ and trifluoroethanol and pyrazole, respectively.

Although the present structure describes an abortive ternary complex, productive binding with the pro-*R* hydrogen toward the nicotinamide ring can easily be obtained by a rotation of *p*-bromobenzyl alcohol along the axis formed by the C7 and bromine atom of the substrate. It is difficult to conceive direct substrate binding to the catalytic metal ion in an abortive complex and outer sphere binding in the catalytically competent complex. The crystallographic studies of substrate binding to the native enzyme (Cedergren-Zeppezauer et al., 1982; Eklund et al., 1982) and the present study on the Cd(II) enzyme support strongly a mechanism in which direct substrate binding is an essential part of the catalytic cycle.

In spite of the structural similarities between the native and the Cd(II)-substituted enzyme, large deviations in kinetic and spectroscopic parameters have been observed (Dietrich, 1980; Dunn et al., 1982; Gerber, 1983). The red shift upon binding of the chromophore substrate DACA is less than that in the native and Co(II)- and Ni(II)-substituted enzymes. The specific activity is about 14% of the native enzyme. Differences in the rate of hydride transfer, coenzyme dissociation, and kinetic isotope effects were also found. In an attempt to explain these discrepancies between the native and the Cd(II) enzyme, Dunn et al. (1982) discussed three possible reasons for the different kinetic behavior of the Cd(II) enzyme: Cd(II) is a weaker Lewis acid than Zn(II) and will activate the substrate less efficiently. Due to the larger ionic radius and bond lengths to the ligands, the position of the Cd(II) ion in Cd^{II}-LADH will be shifted compared to the Zn(II), Co(II), and Ni(II) enzymes, bringing about a misalignment of the reacting atoms. Third, a possible five-coordination of the catalytic metal ion in the Cd(II) enzyme in contrast to the other metallo LADH's was discussed. From the results presented here, we believe that five-coordination as primary reason for the deviations in the kinetic parameters can be excluded. The orientation of the Cd(II), nicotinamide ring, and substrate relative to each other in the ternary complex Cd^{II}-LADH/NADH/*p*-bromobenzyl alcohol is highly similar to that of the native ternary complex. Small observed differences are within the error limits of our maps and cannot be described as significant at the present resolution of the maps.

Conclusions

The X-ray crystallographic study of the free Cd(II) enzyme, its binary complex with NADH, and ternary complex with NADH and *p*-bromobenzyl alcohol revealed a high similarity between this derivative and the native enzyme. These results justify the use of Cd^{II}-LADH as a model system for the native enzyme with Cd(II) as a probe in the active site. At the present resolution of the X-ray analysis, differences in kinetic parameters cannot be related to certain significant structural deviations in the Cd(II) enzyme; rather, they must reflect the intrinsic chemical properties of Cd(II) and its different influences on the metal environment as compared to the native protein.

Acknowledgments

We thank Dr. T. A. Jones for access to the phase angles for the orthorhombic enzyme prior to publication and help with the refinement programs. Furthermore, we express our gratitude to Prof. C.-I. Brändén for all the facilities placed at our disposal in Uppsala. We thank Dr. L. Becker and W. Reinle at the Fachrichtung Analytische and Biologische Chemie, Universität des Saarlandes, for the cadmium determinations and Dr. J. Öberg at the Department for Animal Physiology, Swedish University of Agricultural Sciences, for the use of the atomic absorption spectrophotometer. We gratefully acknowledge the assistance by Prof. G. L. Rossi and Dr. E. Bignetti (University of Parma, Italy) during microspectrophotometric measurements on single crystals. Finally, we thank I. Kurland for linguistic corrections of the manuscript.

REFERENCES

Andersson, I. (1980) Dissertation, Universität des Saarlandes, Saarbrücken, FRG.

Andersson, I., Bauer, R., & Demeter, I. (1982) *Inorg. Chim. Acta 67*, 53–59.

Bertini, I., & Luchinat, C. (1983) *Met. Ions Biol. Syst. 15*, 101–156.

Bignetti, E., Rossi, G. L., & Zeppezauer, E. (1979) *FEBS Lett. 100*, 17–22.

Bobsein, R. B., & Myers, J. R. (1981) *J. Biol. Chem. 256*, 5313–5316.

Cedergren, E. S. (1984) Dissertation, The Swedish University of Agricultural Sciences, Uppsala, Sweden.

Cedergren-Zeppezauer, E., Samama, J.-P., & Eklund, H. (1982) *Biochemistry 21*, 4895–4908.

Dalziel, K. (1957) *Acta Chem. Scand. 11*, 397–398.

Dietrich, H. (1980) Dissertation, Universität des Saarlandes, Saarbrücken, FRG.

Dunn, M. F., Dietrich, H., MacGibbon, A. K. H., Koerber, S. C., & Zeppezauer, M. (1982) *Biochemistry 21*, 354–363.

Eklund, H., & Brändén, C.-I. (1983) in *Zinc Enzymes* (Spiro, T. G., Ed.) pp 123–152, Wiley, New York.

Eklund, H., Nordström, B., Zeppezauer, E., Söderlund, G., Ohlsson, I., Boiwe, T., Söderberg, B.-O., Tapia, O., Brändén, C.-I., & Akeson, A. (1976) *J. Mol. Biol. 102*, 27–59.

Eklund, H., Samama, J.-P., Wallén, L., Brändén, C.-I., Akeson, A., & Jones, T. A. (1981) *J. Mol. Biol. 146*, 561–587.

Eklund, H., Plapp, B. V., Samama, J.-P., & Brändén, C.-I. (1982) *J. Biol. Chem. 257*, 14349–14358.

Eklund, H., Samama, J.-P., & Jones, T. A. (1984) *Biochemistry 23*, 5982–5996.

Gerber, M. (1983) Dissertation, Universität des Saarlandes, Saarbrücken, FRG.

Jack, A., & Levitt, M. (1978) *Acta Crystallogr., Sect. A: Cryst. Phys., Diffr., Theor. Gen. Crystallogr. A34*, 931–935.

Jones, T. A. (1978) *J. Appl. Crystallogr. 11*, 268–272.

Jones, T. A. (1982) in *Computational Crystallography* (Sayre, D., Ed.) pp 303–317, Oxford University Press, New York.

Jones, T. A., & Liljas, L. (1984) *Acta Crystallogr., Sect. A: Found. Crystallogr. A40*, 50–57.

Maret, W., Andersson, I., Dietrich, H., Schneider-Bernlöhr, H., Einarsson, R., & Zeppezauer, M. (1979) *Eur. J. Biochem. 98*, 501–512.

Plapp, B. V., Eklund, H., & Brändén, C.-I. (1978) *J. Mol. Biol. 122*, 23–32.

Schneider, G., Eklund, H., Cedergren-Zeppezauer, E., & Zeppezauer, M. (1983a) *Proc. Natl. Acad. Sci. U.S.A. 80*, 5289–5293.

Schneider, G., Eklund, H., Cedergren-Zeppezauer, E., & Zeppezauer, M. (1983b) *EMBO J. 2*, 685–689.

Sussman, J. L., Holbrook, S. R., Church, G. M., & Kim, S. M. (1977) *Acta Crystallogr., Sect. A: Cryst. Phys., Diffr., Theor. Gen. Crystallogr. A33*, 800–804.

Sytkowski, A. J., & Vallee, B. L. (1979) *Biochemistry 18*, 4095–4099.

Zeppezauer, M. (1983) in *Coordination Chemistry of Metalloenzymes* (Bertini, I., Drago, R., & Luchinat, C., Eds.) pp 99–122, Reidel, Dordrecht, The Netherlands.

Zeppezauer, M., Andersson, I., Dietrich, H., Gerber, M., Maret, W., Schneider, G., & Schneider-Bernlöhr, H. (1984) *J. Mol. Catal. 23*, 377–387.